Tenascin C protects aorta from acute dissection in mice

Taizo Kimura[1,2,3], Kozoh Shiraishi[2], Aya Furusho[4], Sohei Ito[4], Saki Hirakata[4], Norifumi Nishida[4], Koichi Yoshimura[1,5], Kyoko Imanaka-Yoshida[6,7], Toshimichi Yoshida[6,7], Yasuhiro Ikeda[1,2], Takanobu Miyamoto[4], Takafumi Ueno[4], Kimikazu Hamano[5], Michiaki Hiroe[8], Kazutaka Aonuma[3], Masunori Matsuzaki[1,2], Tsutomu Imaizumi[4] & Hiroki Aoki[1,4]

[1]Department of Molecular Cardiovascular Biology, Yamaguchi University School of Medicine, [2]Division of Cardiology, Department of Medicine and Clinical Science, Yamaguchi University Graduate School of Medicine, [3]Division of Cardiovascular Medicine, Medical Science for Control of Pathological Processes, Graduate School of Comprehensive Human Science, University of Tsukuba, [4]Cardiovascular Research Institute, Kurume University, [5]Department of Surgery and Clinical Science, Yamaguchi University Graduate School of Medicine, [6]Department of Pathology and Matrix Biology, Mie University Graduate School of Medicine, [7]Mie University Research Center for Matrix Biology, Mie University Graduate School of Medicine, [8]National Center for Global Health and Medicine, Tokyo, Japan.

Acute aortic dissection (AAD) is caused by the disruption of intimomedial layer of the aortic walls, which is immediately life-threatening. Although recent studies indicate the importance of proinflammatory response in pathogenesis of AAD, the mechanism to keep the destructive inflammatory response in check is unknown. Here, we report that induction of tenascin-C (TNC) is a stress-evoked protective mechanism against the acute hemodynamic and humoral stress in aorta. Periaortic application of CaCl$_2$ caused stiffening of abdominal aorta, which augmented the hemodynamic stress and TNC induction in suprarenal aorta by angiotensin II infusion. Deletion of *Tnc* gene rendered mice susceptible to AAD development upon the aortic stress, which was accompanied by impaired TGFβ signaling, insufficient induction of extracellular matrix proteins and exaggerated proinflammatory response. Thus, TNC works as a stress-evoked molecular damper to maintain the aortic integrity under the acute stress.

A cute aortic dissection (AAD) is an abrupt destruction of aortic walls that is immediately life-threatening and is more prevalent than the rupture of abdominal aortic aneurysm (AAA), another life-threatening aortic disease in adult[1]. Although AAD imposes a significant health problem, its molecular pathogenesis is largely unknown except for genetic connective tissue diseases, including Marfan syndrome and Loeys-Dietz syndrome[2], which account for approximately 10% of all AAD cases[1].

Multiple lines of evidence indicates the central role of inflammation in aortic pathology associated with the connective tissue diseases[2]. In these diseases, affected aortic tissue manifests histological abnormalities, including degeneration of extracellular matrix (ECM) and cellular infiltration, which indicate that chronic inflammation precedes the aortic dissection and rupture. As for the animal model of AAD, pathological stress by angiotensin II (AngII) infusion to aged mice induces AAD in an IL-6/MCP-1-dependent manner, underscoring the importance of the proinflammatory response[3]. However, common form of human AAD is characterized by the disruption of the intimomedial layer of aortic walls that otherwise show minimal histological abnormalities[1], suggesting that chronic inflammation alone may not explain the pathogenesis of common AAD.

Although hypertension is a known risk for human AAD, high blood pressure alone does not result in the destructive inflammatory response of aorta in most people. Likewise, AngII infusion into young mice does not cause AAD or other destructive inflammatory response[4]. These facts suggest the presence of a protective mechanism to keep the destructive inflammatory response in check to maintain the integrity of the aortic walls under the stress. Although such a protective mechanism of aortic walls, if exists, may be involved in pathogenesis of AAD, its molecular nature is unknown.

During the investigation into the role of a matricellular protein tenascin C (TNC) in AAA pathogenesis[5], we serendipitously discovered that TNC is involved in pathogenesis of AAD, but not in that of AAA, subsequent to combined insults with periaortic CaCl$_2$ (Ca) treatment[6,7] and AngII infusion. Ca treatment caused stiffening of aorta, a known risk factor for AAD in humans, and augmented the hemodynamic stress and TNC expression by AngII in the aorta. In turn, TNC expression was essential for reinforcing the tissue by the expression of ECM

proteins and for ameliorating an excessive proinflammatory response both in aortic tissue *in vivo* and in aortic smooth muscle cells *in vitro*. Our findings indicate that stress-induced TNC expression is a previously unrecognized protective mechanism in aortic walls, of which failure leads to AAD development.

Results

Development of AAD in TNC-deficient mice. We first investigated the role of TNC in a mouse model of AAA by Ca treatment of the infrarenal aorta[6,7], as we recently found that TNC expression is associated with inflammation and tissue destruction in AAA[5]. However, Ca treatment caused comparable AAA in wild type (WT) and *Tnc*-null (TNC-KO) mice (Supplementary Figs. 1a and 1b) 6 weeks after the Ca treatment when this model reaches the plateau of AAA growth[7], indicating that TNC did not play a major role in the chronic tissue destruction in this AAA model. We then treated mice with AngII infusion (1,000 ng/min/kg) in addition to Ca (Ca + AngII) to further stress the aortic walls. Ca + AngII caused comparable increase in the systolic blood pressure in WT and TNC-KO mice (Supplementary Fig. 1c). Again, Ca-treated aorta segments from WT and TNC-KO mice showed comparable AAA (Fig. 1a, brackets, Supplementary Fig. 1a, b). Unexpectedly, five of 15 TNC-KO mice showed a striking enlargement of the suprarenal aorta after Ca + AngII (Fig. 1a, arrowheads), even though this part of aorta was not exposed to Ca treatment. An additional two TNC-KO mice died of suprarenal aortic rupture. Thus, nearly half of the TNC-KO mice developed suprarenal aortic lesions, whereas WT mice showed no such lesions (P < 0.01 compared to WT, Fig. 1b). Although AngII alone caused enlargement of the suprarenal aorta in two TNC-KO mice, the incidence was significantly lower than in Ca + AngII mice (P < 0.05).

To better understand the nature of the lesions, we observed the enlarged suprarenal aortae in TNC-KO mice by optical coherence tomography (OCT). The OCT images revealed the "double-barrel" appearance of the true and false lumens that were connected by a narrow channel (Fig. 1c, d, Supplementary Movies 1 and 2), which is a typical finding in human AAD. Ultrasonography of live mice (Supplementary Fig. 2a) also showed the true and false lumens. Histological study demonstrated that the structure of intimomedial layer of the true lumen was largely preserved, but there was an disruption of the medial layer, a hallmark of AAD, in the transition to the fibrous wall of the false lumen (Fig. 1e, Supplementary Fig. 2b). Whereas the intimomedial disruption in human AAD is followed by the longitudinal tearing of the medial layer, the aortic lesions in mice mainly manifested the rupture of aorta and formation of pseudoaneurysm, probably because the medial layer consists of about 100 elastic lamellae in human but only 3–4 elastic lamellae in mice. From these findings we concluded that TNC-KO developed AAD, which recapitulate the intimomedial disruption as observed in human AAD, upon the Ca + AngII treatment.

Synergistic augmentation of hemodynamic stress and TNC expression by Ca + AngII. Although others reported that AngII infusion (2,500 ng/min/kg) causes AAD in old mice (7–12 months old)[3], AngII (1,000 ng/min/kg) alone in younger WT mice (10–14 weeks of age) did not induce an obvious AAD in our hands (Fig. 1a, b). This raises two questions: (1) Why does infrarenal Ca treatment influence AAD development in the distant suprarenal aorta in TNC-KO mice? (2) How is TNC involved in AAD pathogenesis? Aortae with AAD showed an intact segment (Fig. 1a, double arrow) between the Ca-treated segment (Fig. 1a, bracket) and AAD (Fig. 1a, arrowheads), suggesting that direct propagation of Ca-induced tissue destruction was unlikely to have caused suprarenal AAD. Serum cytokine levels in WT mice showed no significant changes 6 weeks after the AngII or Ca + AngII treatment (Supplementary Fig. 3), indicating an absence of generalized inflammation in this setting.

We reasoned that Ca treatment might cause aortic stiffening, a known risk factor for AAD in humans[8,9], by inducing periaortic fibrosis and loss of the spring-like elastic lamellae structures (Fig. 2a, b and Supplementary Fig. 1a). The stiffening of the infrarenal aorta would then augment the hemodynamic stress on the suprarenal aorta due to the loss of the Windkessel effect[10]. Indeed, the pressure-diameter (PD) curve of excised aortae after Ca + AngII treatment showed a marked downward shift, indicating stiffening in the infrarenal aorta, whereas that of the suprarenal aorta showed no change (Fig. 2c). Hemodynamic measurements by aortic catheterization in live mice indicated that one week of Ca + AngII treatment increased dP/dt (Fig. 2d) at comparable blood pressures (Supplementary Fig. 4a). Ultrasonography performed in live 1 week after the Ca + AngII treatment revealed a reduction in the systolic descent rate of the infrarenal aorta and an augmentation of that of the suprarenal aorta (Supplementary Fig. 4b).

As *Tnc* is a mechanosensitive gene[11,12], we examined its expression using the *Tnc* reporter mice in which *lacZ* was knocked into one of the *Tnc* loci[13]. In control mice without Ca or AngII treatment, *Tnc* expression was restricted to the lower aorta (Fig. 2e, Supplementary Fig. 5a) where dP/dt was higher than the upper aorta (Fig. 2d). Infrarenal Ca treatment induced *Tnc* expression in the infrarenal aorta[5], and systemic AngII infusion resulted in *Tnc* expression in the entire aorta (Supplementary Fig. 5a). Ca and AngII treatments synergistically enhanced and prolonged *Tnc* expression in the upper aorta (Fig. 2e, Supplementary Fig. 5a), probably due to the augmented hemodynamic stress (Fig. 2d). Histological analysis revealed that TNC was expressed by the smooth muscle α-actin positive cells, most likely smooth muscle cells, in the medial layer (Supplementary Fig. 5b). The synergy of Ca and AngII in enhancing *Tnc* gene expression was reflected in the increase in serum TNC levels 6 weeks after the treatment of WT mice (Supplementary Fig. 5c). Therefore, Ca treatment caused the stiffening of the infrarenal aorta and augmented AngII-induced hemodynamic stress and *Tnc* expression.

Transcriptome analysis before AAD development. We next investigated how TNC was involved in the pathogenesis of AAD. Serial ultrasonography in TNC-KO mice revealed that AAD developed after 10–15 days of Ca + AngII treatment. We performed a transcriptome analysis 1 week after starting Ca + AngII in the suprarenal aorta; at this time, there was no obvious AAD. The Ca + AngII-induced genes comprised 1,115 probe sets with z scores > 2 in either WT or TNC-KO mice. Analysis using Database for Annotation, Visualization and Integrated Discovery (DAVID)[14] identified a functional annotation cluster with the highest enrichment score (28.54) with the gene ontology terms "extracellular region," "extracellular region part" and "extracellular space," which contained 182 probe sets (Fig. 3). Hierarchical average linkage clustering of these probe sets revealed distinct subclusters. Subcluster #1, which was induced strongly in WT mice but weakly in TNC-KO mice, contained genes encoding ECM proteins, including elastin, collagens, fibrillin-1 and fibulins, which are essential for aortic tissue integrity[2,15]. Subcluster #2, induced weakly in WT mice but strongly in TNC-KO mice, contained genes encoding proinflammatory cytokines and chemokines, which are reportedly involved in pathogenesis of mouse AAD[3]. Other functional annotation clusters also indicated an ineffective induction of ECM genes and an exaggerated proinflammatory response in TNC-KO mice (Supplementary Fig. 6a–d).

Mechanism of TNC-mediated aortic protection. We confirmed the exaggerated proinflammatory response by quantitative RT-PCR in the suprarenal aorta of TNC-KO mice 1 week after the Ca + AngII treatment (Fig. 4a, Supplementary Fig. 7a). As TNC is expressed in medial smooth muscle cells (Supplementary Fig. 5b), we examined the TNC in aortic smooth muscle cells in culture. We cultured suprarenal aortic smooth muscle cells from TNC-KO mice in the

2
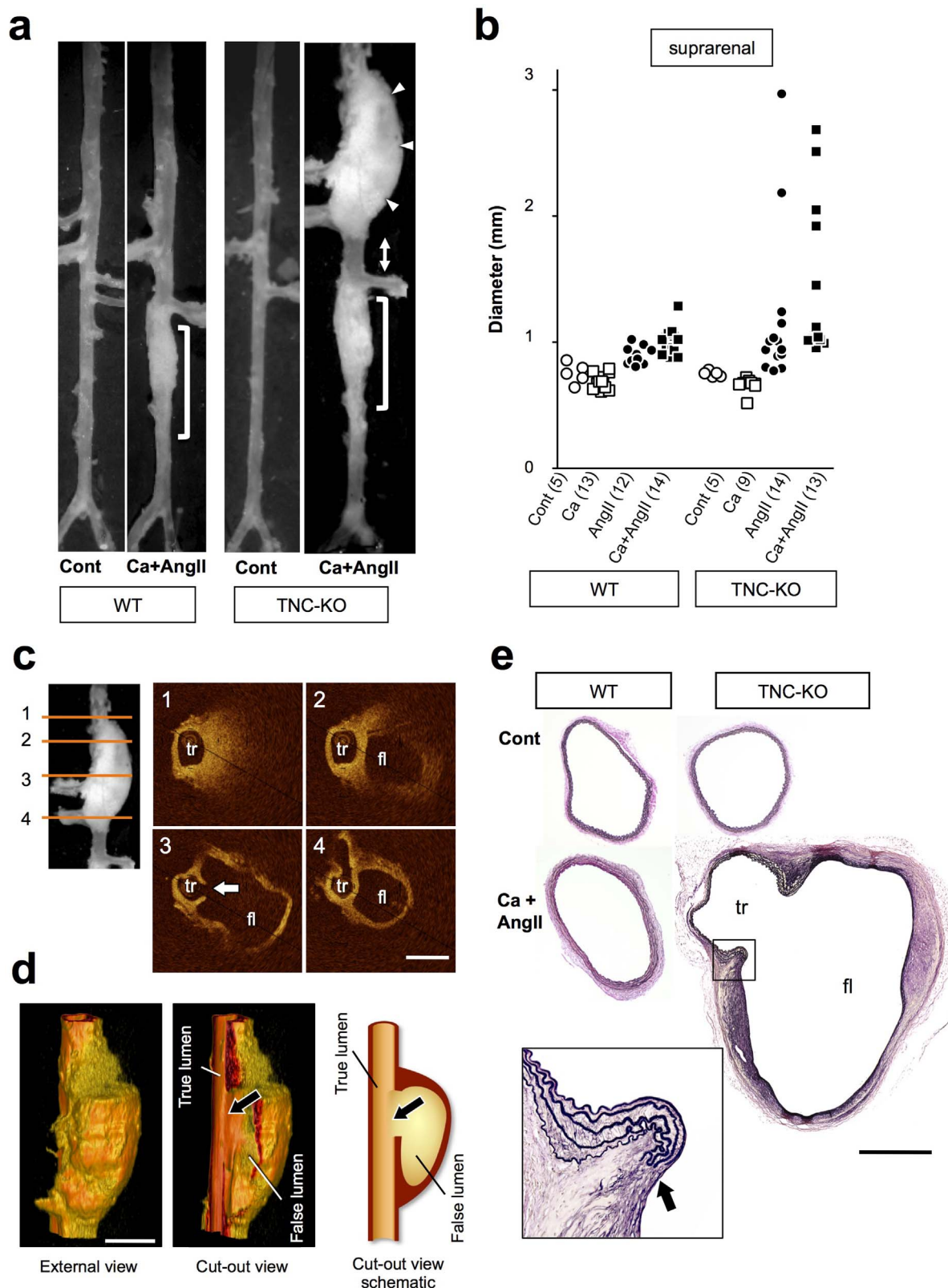
Figure 1 | Aortic dissection elicited by Ca + AngII treatment in TNC-KO mice. (a) Representative images of aortae from WT and TNC-KO mice. Brackets indicate the Ca-treated segments. Arrowheads and a double arrow indicate the enlarged and normal segment of the TNC-KO aorta, respectively. (b) Diameters of suprarenal aortae from WT or TNC-KO mice with the indicated treatment. Animal numbers are indicated in parentheses. (c), (d) Representative images of optical sections (c) and 3D reconstruction (d) by optical coherence tomography of an enlarged TNC-KO aorta. Arrows indicate the dissection of the aortic wall. (e) Elastica van Gieson (EVG) staining of suprarenal aortae from WT and TNC-KO mice. The inset shows an enlarged image of the area in the square. The arrow points to the disrupted medial layer. True (tr) and false (fl) lumens of the aorta are indicated. Bars, 0.5 mm.
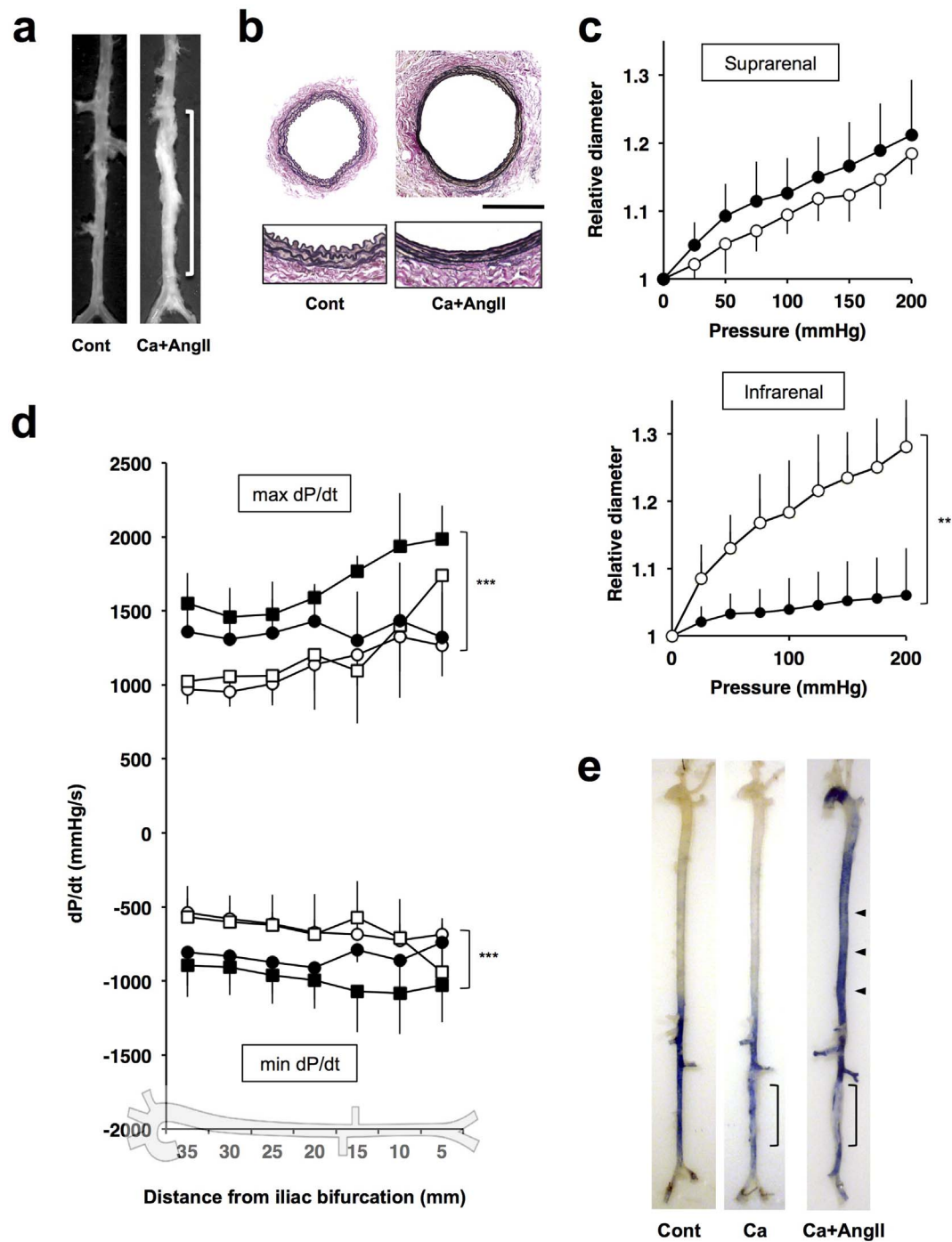
Figure 2 | Aortic stress elicited by Ca + AngII treatment. Representative photographs (a) and EVG staining (b) of infrarenal aortae without (Cont) and with Ca + AngII treatment. The bracket indicates the Ca-treated region. Bar, 0.5 mm. (c) Pressure-diameter (PD) curves of the suprarenal (upper panel) and the infrarenal (lower panel) regions of the aortae are shown for untreated controls (open circles) and 6 weeks after Ca + AngII treatment (closed circles). Data, which are expressed relative to the aortic diameter at 0 mmHg, are the mean ± standard deviation (SD) of four independent observations for each group. (d) Maximum and minimum dP/dt of the pressure wave is shown for control (open circles), Ca treatment (open squares), AngII treatment (closed circles) and Ca + AngII treatment (closed squares) after 1 week of treatment at various positions in the aortae, as illustrated at the bottom of the panel. Data are the mean ± SD of eight independent observations. **P < 0.01 and ***P < 0.001 compared to control. (e) β-galactosidase staining of *Tnc* reporter mice aortae with or without 6 weeks of Ca + AngII treatment. Brackets indicate the Ca-treated segment. Arrowheads indicate enhanced β-galactosidase activity.

presence or absence of exogenous TNC and then stimulated them with TNFα to investigate the cellular response to the proinflammatory environment. Quantitative RT-PCR revealed that a higher proinflammatory response was elicited by TNFα in the absence of exogenous TNC (Fig. 4b, Supplementary Fig. 7b). TNFα also suppressed many of the collagen family genes[16], which was partially prevented by exogenous TNC (Supplementary Fig. 7c), suggesting that the presence of TNC supported the expression of the collagen family genes. Therefore, deletion of *Tnc* resulted in the exaggerated the proinflammatory response and the ineffective induction of ECM genes in aortic tissue *in vivo* and in aortic smooth muscle cells *in vitro*.

Annotation Cluster 1 Enrichment Score: 28.54
GOTERM_CC_FAT   GO:0005576~extracellular region
GOTERM_CC_FAT   GO:0044421~extracellular region part
GOTERM_CC_FAT   GO:0005615~extracellular space
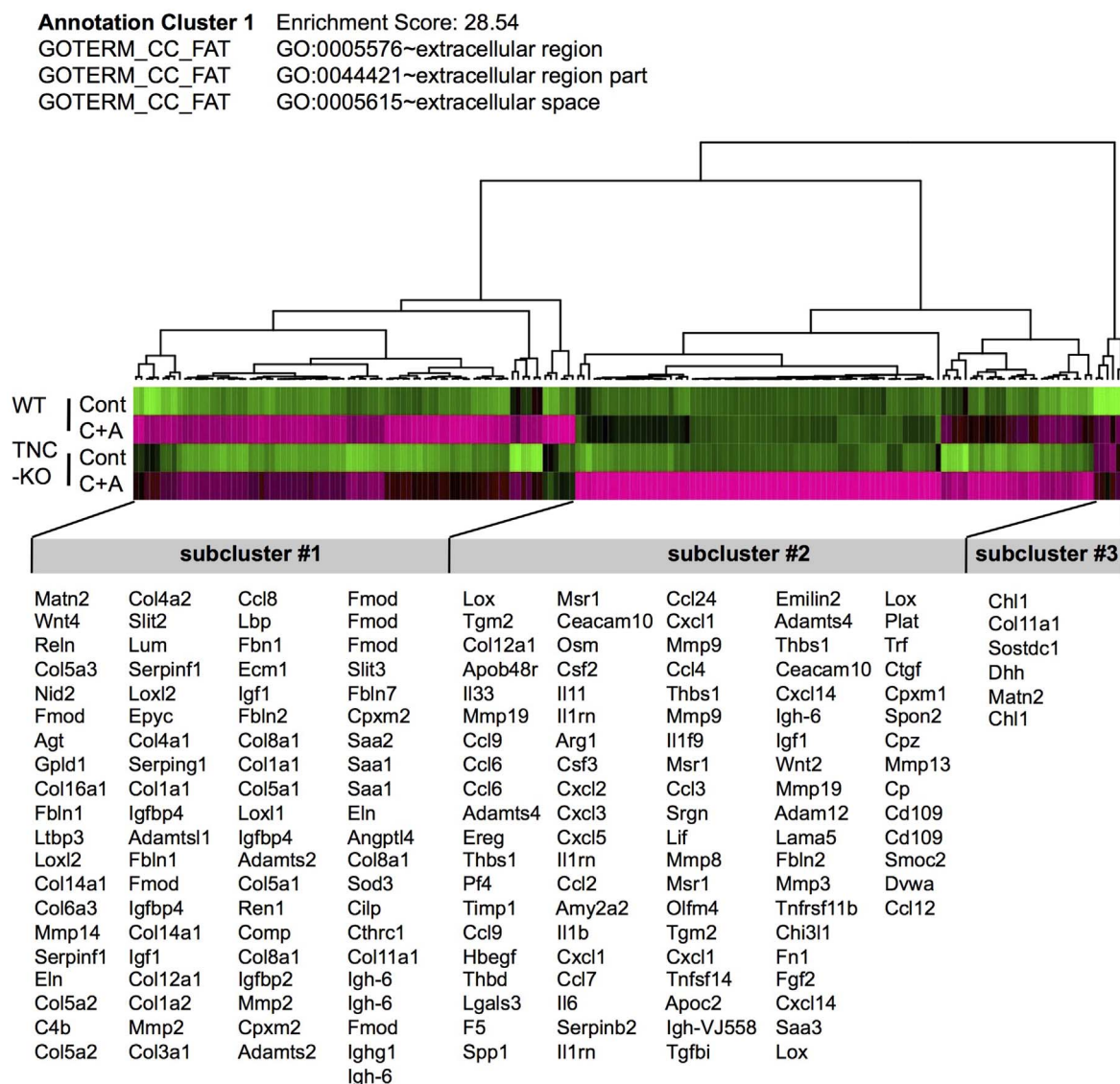
Figure 3 | Transcriptome of the mouse aorta before dissection. Heat map diagram of average linkage hierarchical clustering of the genes induced by Ca + AngII in WT and in TNC-KO mice. The functional annotation cluster is shown with the highest enrichment score by DAVID analysis. RNA samples were from WT or TNC-KO mice with (C + A, n = 8) or without (Cont, n = 5) Ca + AngII treatment for 1 week.

Induction of proinflammatory genes, including IL-6 and CCL-2 (MCP-1), before AAD development is consistent with a previous report[3]. On the other hand, the impact of the suppression of ECM genes in this experimental setting was to be investigated. Picrosirius red staining of the suprarenal aorta revealed that medial collagen deposition did not differ between untreated WT and TNC-KO mice (Fig. 4c, Supplementary Figs. 8a and 8b), consistent with the notion that TNC is dispensable for the normal development[13]. While 1 week of Ca + AngII treatment was associated with an increase in medial collagen deposition in WT mice, the response was weaker in TNC-KO mice (Fig. 4c). Obvious changes in adventitial sirius red staining was not observed (Supplementary Fig. 8b), possibly because collagen was already abundant in samples without Ca + AngII treatment. The increase in medial collagen deposition in WT by Ca + AngII treatment was accompanied by the increase in the immunoreactivity of type I collagen (Fig. 4d, Supplementary Fig. 8c). Immunoreactivity of lysyl oxidase, a cross-linking enzyme for collagen and elastin, showed a decrease by Ca + AngII treatment whereas that of fibronectin showed no obvious change (Supplementary Fig. 8c), although the expressions of their genes were increased by Ca + AngII treatment

(Fig. 3). This may be due to the post translational regulation of protein levels as recently reported for lysyl oxidase[17].

The PD curve of the suprarenal aorta from untreated TNC-KO mice overlapped with that of WT mice (Fig. 4e), indicating that TNC is dispensable for the normal biomechanics of the aorta. The PD curve 1 week after the Ca + AngII treatment showed a mild but significant (P < 0.05) upward shift in WT mice. In TNC-KO mice, Ca + AngII treatment caused a more prominent upward shift of the PD curve (P < 0.001 compared with WT control), suggesting a greater loss of wall strength than in WT mice. Notably, the PD curve of the Ca + AngII-treated WT suprarenal aortae at 6 weeks returned to that of the untreated control, suggesting a recovery of once-lost wall strength.

Cellular response in aorta before AAD development. To better understand the cellular responses in the aorta before the AAD development, we took advantage of the imaging cytometry that can analyze the intracellular signal response at the single cell levels in the context of the aortic tissue. We obtained suprarenal aortic tissue from WT or TNC-KO mice 1 week after the Ca + AngII
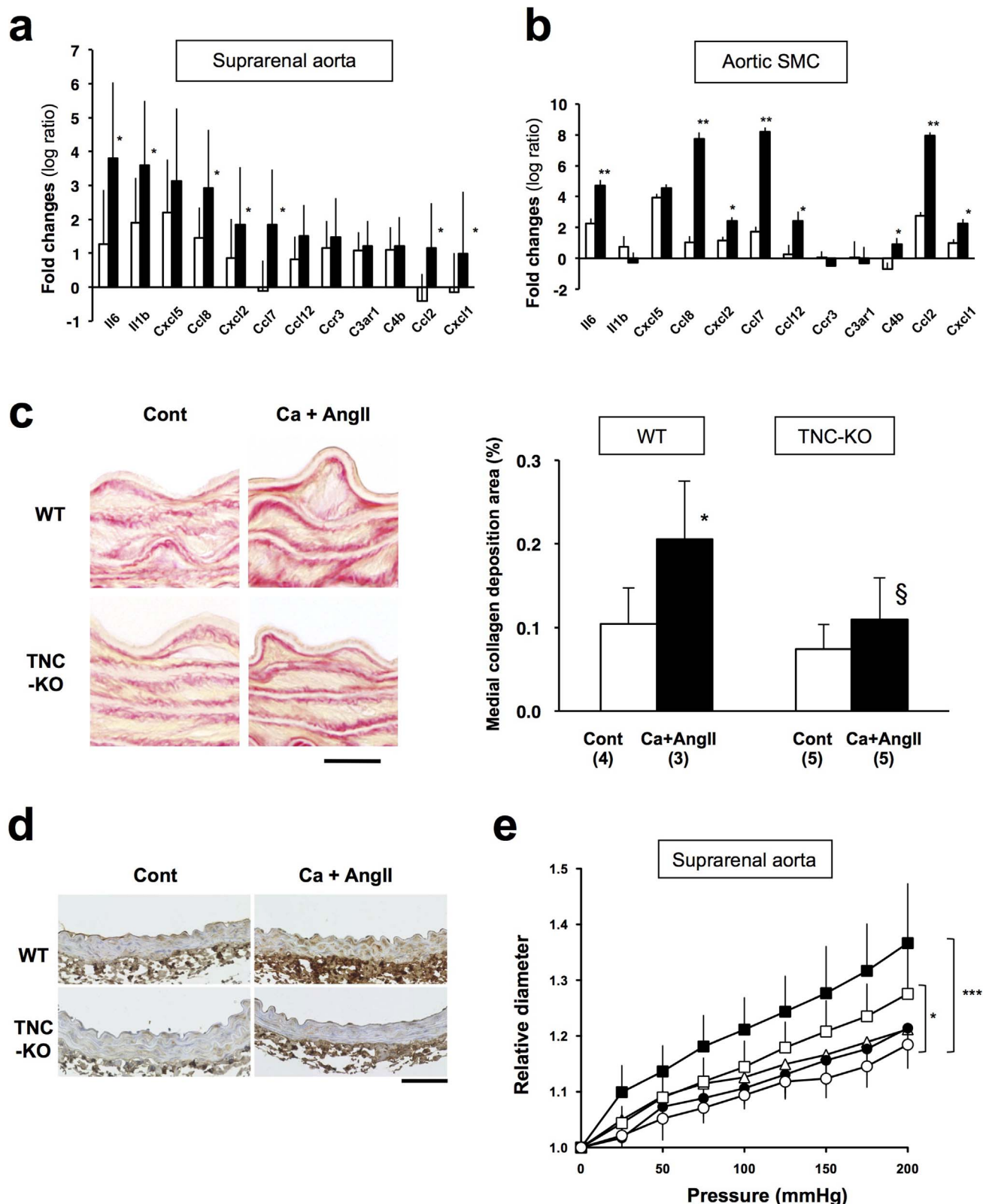
Figure 4 | Stress response of the mouse aorta before dissection. (a) Fold induction of proinflammatory genes in the suprarenal aorta of WT (open columns) or TNC-KO mice (closed columns) after 1 week of Ca + AngII treatment. Shown are the 12 genes with the highest induction in TNC-KO aortae out of 84 proinflammatory genes using a commercially available PCR array. (b) Genes induced by 10 ng/mL TNFα in TNC-KO aortic smooth muscle cell (SMC) culture in the presence (white) or absence (black) of exogenous TNC (10 μg/mL). Data are the mean ± SD of eight independent observations. *P < 0.05 and **P < 0.01 compared to those with TNC. (c) Picrosirius red-stained medial layer of suprarenal aorta in WT and TNC-KO mice with or without Ca + AngII treatment for 1 week. Bar, 10 μm. Data are the mean ± SD of five independent observations. *P < 0.05 compared to WT control. §P < 0.05 compared to WT Ca + AngII. (d) Representative images of type I collagen immunostaining are shown for WT and TNC-KO aortae with or without 1 week of Ca + AngII treatment. Bar, 50 μm. (e) PD curves of the suprarenal regions of the excised aortae from WT (open symbols) and TNC-KO (closed symbols) mice treated with (squares) or without (circles) Ca + AngII for 1 week. Open triangles indicate WT with Ca + AngII for 6 weeks. Data are the mean ± SD of seven independent observations. *P < 0.05 and ***P < 0.001 compared to WT control.
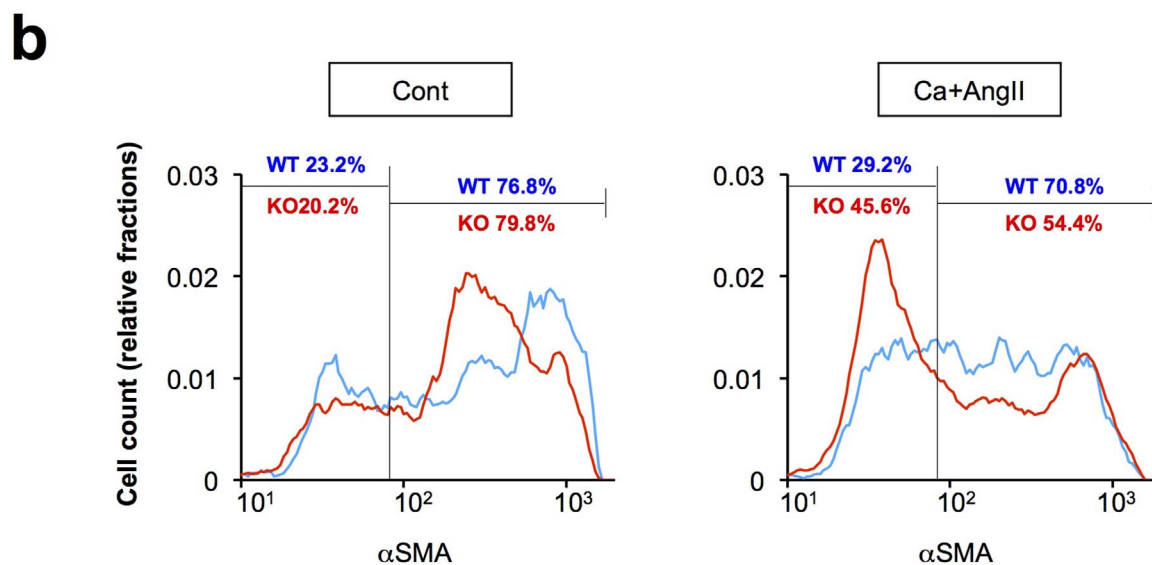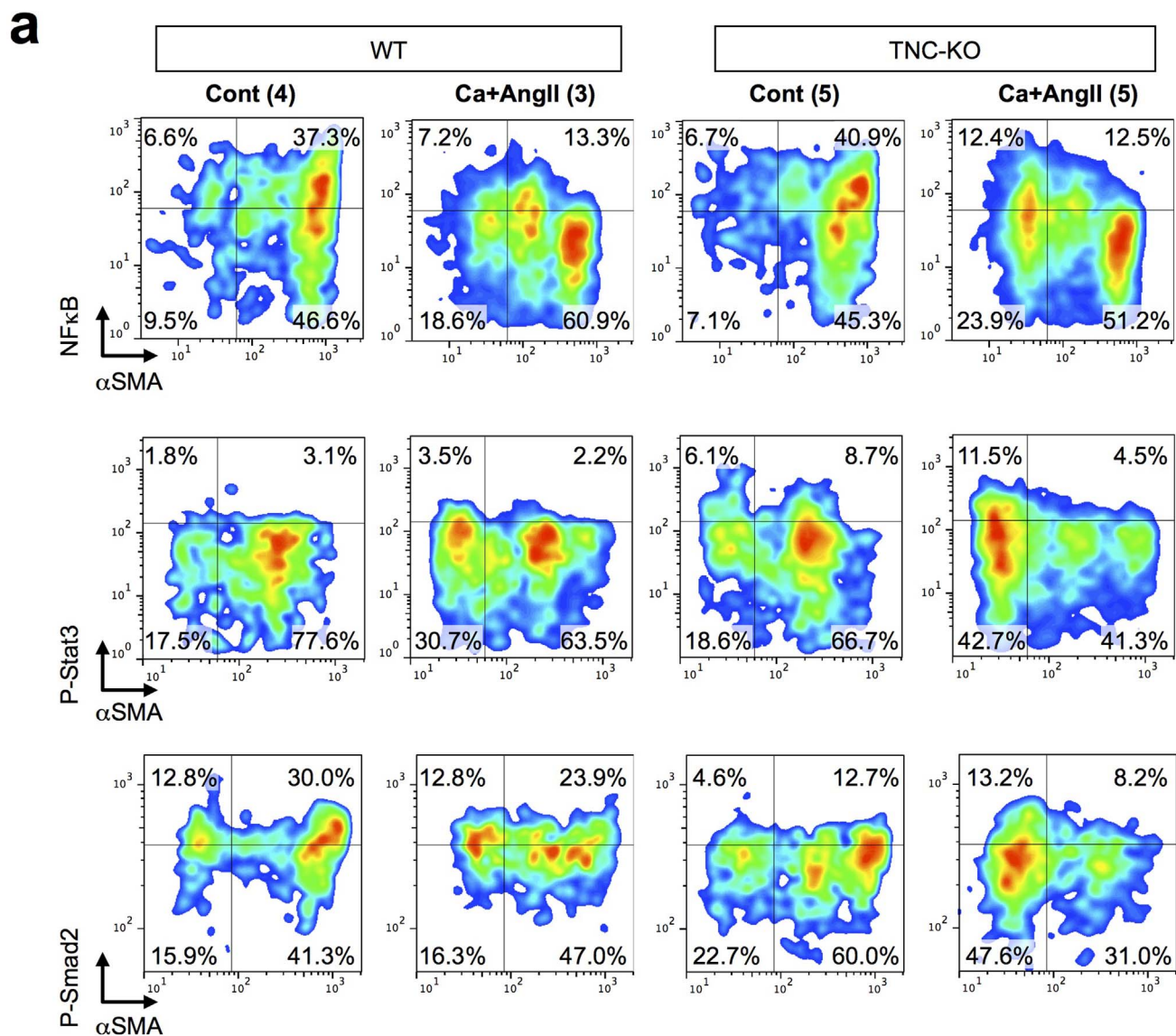
Figure 5 | Cellular responses in mouse aorta before AAD development. (a) Imaging cytometric analyses of aortae. Scattergrams are shown for the fluorescence intensities of NFκB, phospho-Stat3 (P-Stat3) and phospho-Smad2 (P-Smad2) immunostainings, along with that of smooth muscle α-actin (αSMA). Aortae were obtained from WT or TNC-KO mice with or without 1 week of Ca + AngII treatment. Animal numbers are indicated in parentheses. (b) Analyses of αSMA intensities. Blue and red lines indicate the histograms of WT and TNC-KO (KO), respectively.

treatment or without Ca + AngII treatment and analyzed for smooth muscle α-actin (αSMA), nuclear NFκB, phospho-Stat3, phospho-Smad2 and CD45 (Fig. 5, Supplementary Figs. 9 and 10). Double labeling for αSMA and CD45 revealed that the majority of the αSMA-negative cells were CD45-positive inflammatory cells (Supplementary Fig. 9). Ca + AngII treatment caused slight increases in nuclear NFκB (from 6.6% to 7.2%) and phosho-Stat3 (from 1.8% to 3.5%), the major transcription factors for proinflammatory signaling, in αSMA-negative cells of WT aorta (Fig. 5a). Ca + AngII caused more prominent increases in nuclear NFκB (from 6.7% to 12.4%) and phosho-Stat3 (from 6.1% to 12.4%) in αSMA-negative cells of TNC-KO aorta, consistent with the exaggerated proinflammatory response. In contrast, nuclear phospho-Smad2, the downstream of TGFβ signal, was weaker in TNC-KO aorta both in αSMA-positive and -negative populations regardless of Ca + AngII treatment (Fig. 5A, Supplementary Fig. 10). Interestingly, although the ratio of αSMA-positive cells in total cell populations was comparable between WT and TNC-KO aortae without Ca + AngII treatment, TNC-KO aorta showed weaker expression αSMA (Fig. 5b). TNC-KO aorta showed more increase in the proportion of αSMA-negative cells, presumably CD45-positive inflammatory cells, than WT aorta by Ca + AngII treatment (Supplementary Fig. 9). This could be due to actual increase in αSMA-negative cells, decrease in αSMA-positive cells, or both. Further studies would be required to evaluate the effect of TNC on infiltration, survival and proliferation of various cell types. Taken together, reduced TGFβ signaling may underlie the abnormal response of TNC-KO aorta, including compromised tissue reinforcing response[18], reduced αSMA expression[19] and exaggerated proinflammatory response in aorta.

Discussion

In this study, we provided a new model of aortic stiffening, a known risk factor for AAD[8–10,20], that augments the hemodynamic stress elicited by AngII. Using this model, we demonstrated that TNC protects the aorta from AAD, but not from AAA, via two mechanisms. First, TNC supports the stress-induced expression of ECM that reinforce the aorta[21]. Second, TNC expression dampens the stress-induced excessive inflammatory response in the aorta (Fig. 6).

Although induction of TNC is associated with deposition of ECM during the inflammatory responses in cardiovascular[5,22] and other tissues with high mechanical stress[23], its significance in stress adaptation has been unclear. Our data indicate that TNC acts as a stress-evoked molecular damper that keeps the destructive stress response in check before AAD development (Fig. 4e). Exaggerated inflammatory response with higher IL-6 expression in the absence of TNC has also been reported in the brain injury model[24]. In addition, IL-6 has been reported to play a crucial role in AAD development[3].

It is noteworthy that *Tnc* deletion augmented NFκB and Stat3 activities mainly in αSMA-negative cells, most of which were CD45-positive inflammatory cells (Supplementary Figs. 9 and 10). On the other hand, *Tnc* deletion diminished Smad2 activity in both αSMA-positive and -negative cells. This cell type-specific effect of *Tnc* deletion could be due to a number of factors, including changes in the cytokine environment and the sensitivity of a cell type to cytokines, which could be modulated by TNC. The diminished Smad2 activity indicates the impaired TGFβ signaling that regulates ECM biosynthesis[18] and smooth muscle differentiation[19] in TNC-KO aorta. Consistently, TNC-KO aorta showed reduction in basal αSMA expression and impairment of ECM gene inductions in response to the aortic stress, suggesting that TNC is involved in the normal function of aortic smooth muscle cells as proposed in the developing coronary arteries[25]. Thus, reduction in TGFβ signaling may be the underlying mechanism for AAD development in TNC-KO. Interestingly, genetic defect in tenascin-X, a constitutively expressed member of tenascin family, causes a recessive form of Ehlers-Danlos syndrome because of insufficient deposition of ECM and reduction
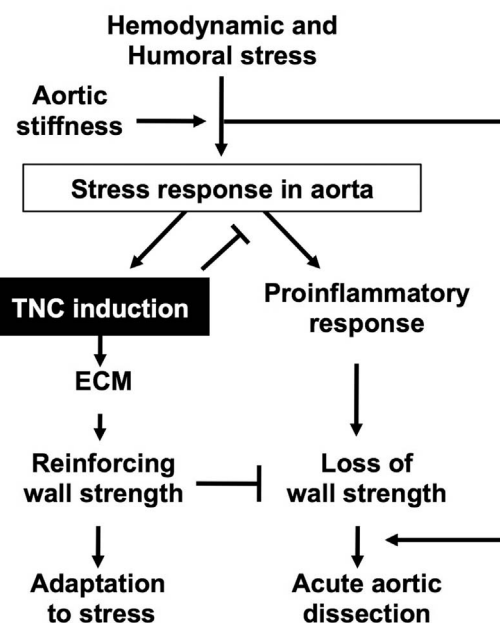
Figure 6 | **Schematic diagram of TNC-mediated protection of the aorta.** Aortic stress induces TNC expression, which in turn protects the aorta by reinforcing the wall strength of the aortic tissue and by suppressing an excessive proinflammatory response.

in the tensile strength of the affected tissue[26]. TNC may function in the analogous way with tenascin-X in the tissue under high mechanical stress by facilitating the deposition of ECM to reinforce the tissue.

The limitation in this study is the different manifestation of AAD in mouse and human. The mouse AAD in this study showed the disruption of normally-looking intimomedial layer that recapitulates the pathological hallmark of human AAD. However, the mouse AAD did not recapitulate the longitudinal dissection of medial layers that follows the intimomedial layer disruption in human. This is most likely because the aortic wall in human consists of tens of elastic lamellar units whereas that of mice consists of only 3 to 4 units. Thus, disruption of a few elastic lamellar units results in the complete rupture of aorta rather than the tearing of medial layer. The progression of AAD subsequent to the intimomedial disruption would require future investigation, possibly in larger animals. Another difference is that most of human AAD develops in thoracic aorta, whereas most of the mouse AAD developed in suprarenal aorta in this and other studies[3,27]. A number of potential reasons for this could be considered, including the different hemodynamics in human and mouse, which require further studies. In this regard, it is noteworthy that intrinsic TNC expression is low in part of the ascending and descending aorta, the regions frequently affected in human AAD[1], even under the aortic stress with Ca + AngII treatment. The sharp boundary of the TNC expression pattern suggests the genetically programmed regulation. Whether human aorta have similar expression pattern of TNC, and how TNC expression is regulated in aorta also require future investigation.

Our data demonstrated that aortic stiffening augmented AngII-induced hemodynamic stress and stress response, concomitant with the increase in AAD incidence of TNC-KO mice. However, several questions remain to be answered regarding the mechanistic links among the aortic stiffening, hemodynamic stress and AAD development. First, the difference in AAD incidence caused by the aortic stiffening was relatively small, and the reproducibility of this finding should be tested possibly in other models of aortic stiffening. Second, although we used dP/dt as a readout of hemodynamic stress on aortic walls, further studies are required to investigate how aortic stiffening

influences other hemodynamic parameters. Third, it should be explored what types of hemodynamic stress are sensed by which types of cells in aortic walls, and how the stress is transduced to the responses of destructive inflammation and tissue reinforcement. Furthermore, aortic tissue is likely to have multiple mechanisms, in addition to TNC, to maintain the tissue integrity under various stress. Deciphering such protective mechanisms of the stressed aorta will provide insights into the pathogenesis of AAD, which is essential for developing better diagnostic and therapeutic strategies for this lethal disease.

Methods

Animal experiments. We maintained the TNC-KO mice by mating the heterozygous (TNC$^{+/-}$) pairs and performed experiments using the litter mates of TNC$^{+/+}$ (WT) and TNC$^{-/-}$ (TNC-KO) mice with comparable ages; 10–14 weeks of age at the beginning of Ca + AngII treatment. We used periaortic application of 0.5 M CaCl$_2$ to the infrarenal aorta to create a mouse model for stiffened aorta and infused the mice with AngII (1 μg/min/kg) for up to 4 weeks using osmotic minipump (Alzet model 1004) to apply pathological stress to the aorta[7]. Mice were killed by pentobarbital overdose at the indicated time points and blood and tissue samples were collected. The aortic tissue was excised either immediately for protein and mRNA expression analysis or after perfusion and fixation with 4% paraformaldehyde in PBS at physiological pressure for histological analysis. Enlargement of the aorta was defined when the diameter was equal to or exceeded the 1.5× of control aorta (control diameters; WT 0.75 ± 0.08 mm, KO 0.75 ± 0.02 mm). For the pressure-diameter analysis, aortae were excised and cleaned of peri-adventitial tissue without perfusion fixation. We used the Vevo 770 system (VisualSonics) to measure aortic wall motion in fluothane-anesthetized mice. We performed aortic catheterization of the fluothane-anesthetized mice for direct hemodynamic measurements using Mikro-Tip pressure catheters (Millar) and the PowerLab data acquisition system (Data Science Instruments), after adjusting the systolic blood pressure to approximately 100 mmHg at the most distal measurement point (5 mm above the iliac bifurcation).

Ethics statement. All animal experiment was performed in accordance with the guidelines approved by the ethics committees in Yamaguchi University, Kurume University and Mie University.

Cell culture experiments. We obtained suprarenal aortic smooth muscle cells (SMC) for culture from TNC-KO mice to avoid the influence of endogenous TNC. We isolated the SMCs by enzymatic dispersion, plated on the laminin-coated culture plates (20 μg/mL, 2 hrs at room temperature), and maintained them in Dulbecco's modified Eagle medium (DMEM) supplemented with 10% fetal bovine serum. We cultured TNC-KO aortic SMC in the presence or absence of exogenous TNC (10 μg/mL) and stimulated the cells with 10 ng/mL TNFα for 24 h before obtaining total RNA.

Expression analysis and dataset. Serum TNC levels were determined with an ELISA kit (Immuno-Biological Laboratories). Serum cytokine levels were determined with the Bio-Plex system (Bio-Rad). We isolated total RNA using RNeasy (Qiagen) from SMC culture and suprarenal aorta (from the edge of the right renal artery to approximately 7 mm above) cleaned of peri-adventitial loose connective tissue with intact medial and adventitial layers. We performed transcriptome analyses using the GeneChip Mouse Genome 430 2.0 (Affymetrix) and Microarray Analysis Suite (MAS) 5.0. We also performed quantitative reverse transcription-polymerase chain reaction (RT-PCR) using RT^2 Profiler PCR Array System (Qiagen).

Morphological and functional analyses. We obtained high-resolution optical section images of the excised aorta using an optical coherence tomography (OCT) imaging system (Goodman). We used OsiriX Imaging Software (OsiriX) for three-dimensional reconstruction of the optical sections. For pressure-diameter analysis of the aorta, we ligated the branches of the excised aorta and placed it in a PBS bath on the microscope connected to a charge-coupled device camera. We applied 0–200 mmHg of intra-aortic pressure with a syringe and monitored the external diameters of the aorta with the PowerLab data acquisition system. We observed paraffin-embedded sections of aortic tissue with elastica van Gieson (EVG). For the quantitative analysis of collagen deposition, we stained the aortic tissue sections by picrosirius red. Aortic media, as determined by the area between the innermost and outermost elastic lamellae, was manually traced on the computer images. The collagen deposition area, as determined by the picrosirius red staining, and medial area were measured using ImagePro software (Media Cybernetics). We determined the pattern of *Tnc* gene activity by Bluo-Gal staining of aortae from heterozygous *Tnc* reporter mice in which the *LacZ* gene encoding β-galactosidase was knocked-in to one of the *Tnc* loci[13].

Imaging cytometry and immunohistochemistry. We performed imaging cytometric analysis using ArrayScan XTI (Thermo Fisher Scientific) for mouse aortae 1 week after the Ca + AngII treatment. Two aortic tissue sections were obtained from each mouse; WT (control; n = 4, Ca + AngII; n = 3) and TNC-KO (control; n = 5, Ca + AngII; n = 5). The tissue sections were stained for either NFκB (Cell Signaling

Technologies), phospho-Stat3 (P-Tyr705, Cell Signaling Technologies), phospho-Smad2 (P-Ser465/467, Millipore) and CD45 (Abcam) antibodies with TSA labeling kit with AlexaFluor 488 tyramide (Invitrogen). All of the tissue sections were stained for smooth muscle α-actin (αSMA; Sigma-Aldrich) with DyLight 549-labeled secondary antibody (Jackson ImmunoResearch) and nuclei with DAPI. On average 339 cells/mouse were counted to obtain the cytometric data. For αSMA staining, the same staining and image acquisition protocols were used for all of the samples. For NFκB, phospho-Stat3, phospho-Smad2 and CD45, the staining protocols were optimized for individual target molecules, and a constant image acquisition protocol was used within the same target molecule. The cytometric data obtained by ArrayScan XTI were analyzed by FlowJo software. Immunohistochemical stainings were performed for type 1 collagen (LSL), fibronectin (Sigma-Aldrich) and lysyl oxidase (US Biological).

Statistical analysis. All data are expressed as means ± SD. Statistical analysis was performed with Mann-Whitney test for the comparisons of 2 groups, Kruskal-Wallis test for multiple groups and Friedman test for the pressure-dimension analysis. Post test was performed by Dunn's multiple comparison test. The chi-square test was used where appropriate. P < 0.05 was considered to be significant.

1. Cronenwett, J. L. & Johnston, W. *Rutherford's Vascular Surgery.* 7th edn, (Saunders, 2010).
2. Dietz, H. C. TGF-beta in the pathogenesis and prevention of disease: a matter of aneurysmic proportions. *J Clin Invest* **120**, 403–407 (2010).
3. Tieu, B. C. *et al.* An adventitial IL-6/MCP1 amplification loop accelerates macrophage-mediated vascular inflammation leading to aortic dissection in mice. *J Clin Invest* **119**, 3637–3651 (2009).
4. Bush, E. *et al.* CC chemokine receptor 2 is required for macrophage infiltration and vascular hypertrophy in angiotensin II-induced hypertension. *Hypertension* **36**, 360–363 (2000).
5. Kimura, T. *et al.* Tenascin-C is expressed in abdominal aortic aneurysm tissue with an active degradation process. *Pathol Int* **61**, 559–564 (2011).
6. Longo, G. M. *et al.* Matrix metalloproteinases 2 and 9 work in concert to produce aortic aneurysms. *J Clin Invest* **110**, 625–632 (2002).
7. Yoshimura, K. *et al.* Regression of abdominal aortic aneurysm by inhibition of c-Jun N-terminal kinase. *Nat Med* **11**, 1330–1338 (2005).
8. Khau Van Kien, P. *et al.* Mapping of familial thoracic aortic aneurysm/dissection with patent ductus arteriosus to 16p12.2-p13.13. *Circulation* **112**, 200–206 (2005).
9. Nollen, G. J., Groenink, M., Tijssen, J. G., Van Der Wall, E. E. & Mulder, B. J. Aortic stiffness and diameter predict progressive aortic dilatation in patients with Marfan syndrome. *Eur Heart J* **25**, 1146–1152 (2004).
10. Cavalcante, J. L., Lima, J. A., Redheuil, A. & Al-Mallah, M. H. Aortic stiffness: current understanding and future directions. *J Am Coll Cardiol* **57**, 1511–1522 (2011).
11. Mackie, E. J. *et al.* Expression of tenascin by vascular smooth muscle cells. Alterations in hypertensive rats and stimulation by angiotensin II. *Am J Pathol* **141**, 377–388 (1992).
12. Chiquet-Ehrismann, R. & Chiquet, M. Tenascins: regulation and putative functions during pathological stress. *J Pathol* **200**, 488–499 (2003).
13. Saga, Y., Yagi, T., Ikawa, Y., Sakakura, T. & Aizawa, S. Mice develop normally without tenascin. *Genes Dev* **6**, 1821–1831 (1992).
14. Huang da, W., Sherman, B. T. & Lempicki, R. A. Systematic and integrative analysis of large gene lists using DAVID bioinformatics resources. *Nat Protoc* **4**, 44–57 (2009).
15. de Vega, S., Iwamoto, T. & Yamada, Y. Fibulins: multiple roles in matrix structures and tissue functions. *Cell Mol Life Sci* **66**, 1890–1902 (2009).
16. Verrecchia, F., Wagner, E. F. & Mauviel, A. Distinct involvement of the Jun-N-terminal kinase and NF-kappaB pathways in the repression of the human COL1A2 gene by TNF-alpha. *EMBO Rep* **3**, 1069–1074 (2002).
17. Yokoyama, U. *et al.* Prostaglandin E2 Inhibits Elastogenesis in the Ductus Arteriosus via EP4 Signaling. *Circulation* **129**, 487–496 (2014).
18. Bobik, A. Transforming growth factor-betas and vascular disorders. *Arteriosclerosis, thrombosis, and vascular biology* **26**, 1712–1720 (2006).
19. Kumar, M. S. & Owens, G. K. Combinatorial control of smooth muscle-specific gene expression. *Arteriosclerosis, thrombosis, and vascular biology* **23**, 737–747 (2003).
20. Hiratzka, L. F. *et al.* 2010 ACCF/AHA/AATS/ACR/ASA/SCA/SCAI/SIR/STS/SVM guidelines for the diagnosis and management of patients with Thoracic Aortic Disease: a report of the American College of Cardiology Foundation/American Heart Association Task Force on Practice Guidelines, American Association for Thoracic Surgery, American College of Radiology, American Stroke Association, Society of Cardiovascular Anesthesiologists, Society for Cardiovascular Angiography and Interventions, Society of Interventional Radiology, Society of Thoracic Surgeons, and Society for Vascular Medicine. *Circulation* **121**, e266–369 (2010).
21. Curci, J. A., Baxter, B. T. & Thompson, R. W. in *Vascular Surgery* (ed Rutherford, R. B.) 475–492 (Saunders, 2005).
22. Imanaka-Yoshida, K. Tenascin-C in cardiovascular tissue remodeling: from development to inflammation and repair. *Circ J* **76**, 2513–2520 (2012).

23. Carey, W. A., Taylor, G. D., Dean, W. B. & Bristow, J. D. Tenascin-C deficiency attenuates TGF-beta-mediated fibrosis following murine lung injury. *Am J Physiol Lung Cell Mol Physiol* **299**, L785–793 (2010).
24. Ikeshima-Kataoka, H., Shen, J. S., Eto, Y., Saito, S. & Yuasa, S. Alteration of inflammatory cytokine production in the injured central nervous system of tenascin-deficient mice. *In Vivo* **22**, 409–413 (2008).
25. Ando, K. *et al.* Tenascin C may regulate the recruitment of smooth muscle cells during coronary artery development. *Differentiation* **81**, 299–306 (2011).
26. Burch, G. H. *et al.* Tenascin-X deficiency is associated with Ehlers-Danlos syndrome. *Nature genetics* **17**, 104–108 (1997).
27. Shen, Y. H. *et al.* AKT2 confers protection against aortic aneurysms and dissections. *Circulation research* **112**, 618–632 (2013).

Acknowledgments

Author contributions

T.K., K.Y., A.F., S.I., S.H. and N.N. performed the animal experiments. K.S. and Y.I. performed the aortic catheterization. K.I.-Y. and T.Y. maintained the TNC-KO mice and performed the histopathological analyses. T.U. performed the optical coherence tomography. T.M. performed the bioinformatic analysis. K.H., M.H., K.A., M.M. and T.I. provided scientific advice. H.A., K.Y., K.I.-Y. and M.H. designed this study. H.A. wrote the manuscript.

Additional information